Stem Cell Reports, Volume *13*

Supplemental Information

Effects of Spaceflight on Human Induced Pluripotent Stem Cell-Derived Cardiomyocyte Structure and Function

Alexa Wnorowski, Arun Sharma, Haodong Chen, Haodi Wu, Ning-Yi Shao, Nazish Sayed, Chun Liu, Stefanie Countryman, Louis S. Stodieck, Kathleen H. Rubins, Sean M. Wu, Peter H.U. Lee, and Joseph C. Wu

Inventory of Supplemental Information

Figure S1. Additional hiPSC-CM calcium handling parameters. Related to Figure 3. This figure presents additional calcium imaging data from the analysis shown in Figure 3.

Figure S2. hiPSC-CM gene expression. Related to Figure 4. This figure presents PCR validation and additional analysis of the RNA-sequencing data shown in Figure 4.

Table S1. Differentially Expressed Genes in Multi-Group Comparison. Related to Figure 4. This table contains the expression data for the differentially expressed genes in the heat map in Figure 4A.

Table S2. Motif Enrichment Analysis. Related to Figure 4. This table contains the complete data for motif enrichment analysis, which was used to identify the transcription factors presented in Figures 4C and 4D.

Table S3. DAVID Functional Annotation Clustering. Related to Figure 4. This table contains complete data for the functional annotation clustering represented in Figure 4E.

Video S1. Representative flight contractility at 1.5 weeks. Related to Figure 3. A representative video used for contractility analysis displayed in Figures 3A-C.

Video S2. Representative ground contractility at 1.5 weeks. Related to Figure 3. A representative video used for contractility analysis displayed in Figures 3A-C.

Supplemental Figures

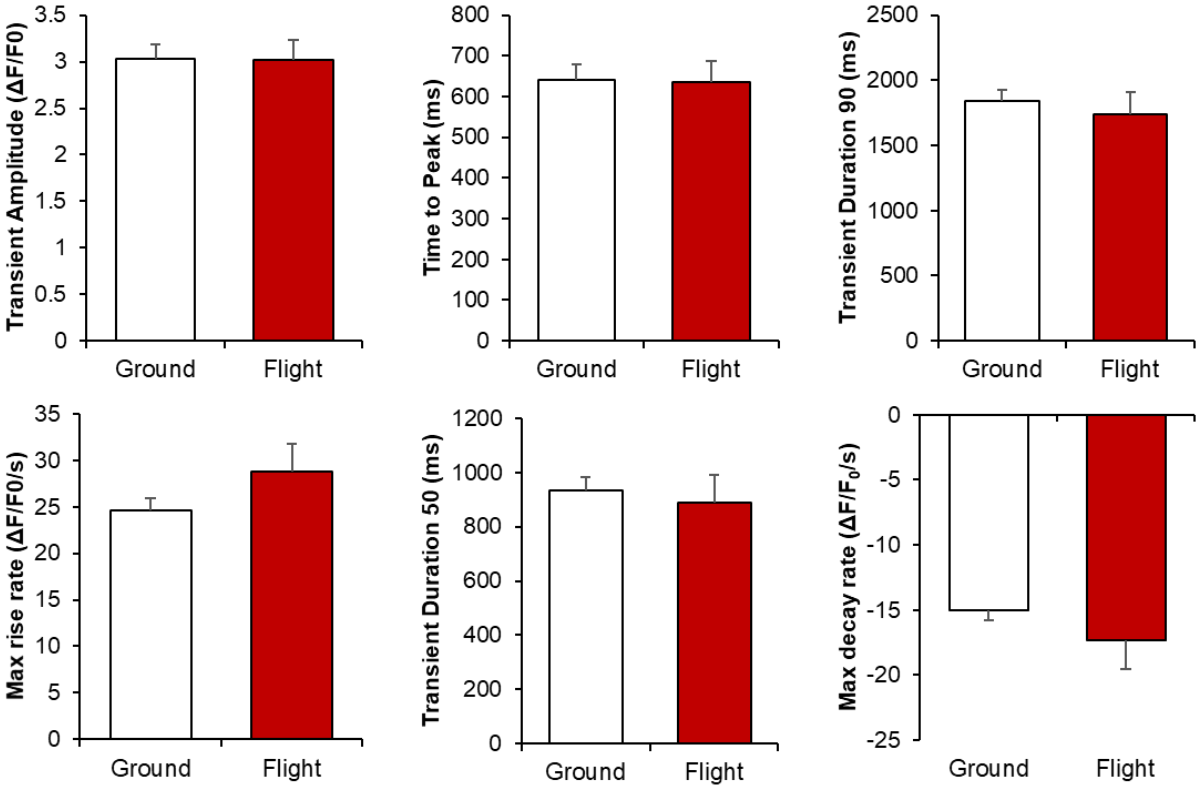

Figure S1. Additional hiPSC-CM calcium handling parameters. Related to Figure 3. Calcium transients were measured in flight and ground control hiPSC-CMs 3 days after live-return from the ISS and were used to calculate calcium handling parameters. N = 103 and 34 cells in ground and flight groups, respectively. Error bars represent standard error of the mean.

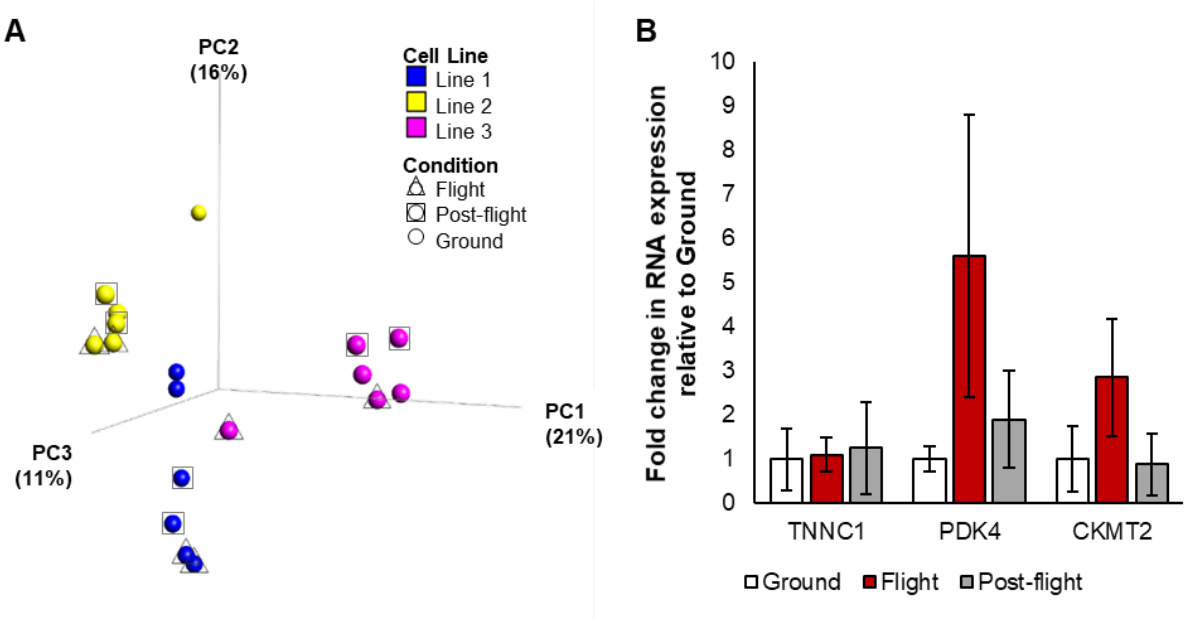

Figure S2. hiPSC-CM gene expression. Related to Figure 4. (A) PCA plot representing gene expression for each sample analyzed. Samples grouped more by cell line than by flight vs ground condition. **(B)** Fold-change in RNA expression of genes in "mitochondria, transit peptide" functional annotation category highlighted in Figure 4E as measured by quantitative PCR. Expression data were averaged by line and then by condition. Error bars represent standard error of the mean.

Supplemental Experimental Procedures

Differentiation of hiPSC-CMs. Three hiPSC lines were generated using a previously published Sendai virus reprogramming protocol on peripheral blood mononuclear cells from three healthy individuals (Churko et al., 2013). These hiPSC lines were differentiated into hiPSC-CMs using a 2D monolayer differentiation protocol and were maintained in a 5% CO_2/air environment as previously described (Lian et al., 2012; Sun et al., 2012). Briefly, hiPSC colonies were dissociated with 0.5 mM EDTA into single-cell suspension and resuspended in E8 media (Life Technologies) containing 10 μM Rho-associated protein kinase inhibitor (Sigma). Approximately 100,000 cells were replated into 6-well dishes pre-coated with Matrigel (BD Biosciences). Next, hiPSC monolayers were cultured to 85% cell confluency. Cells were then treated for 2 days with 6 μM CHIR99021 (Selleck Chemicals) in RPMI 1640+B27 supplement without insulin to activate Wnt signaling and induce mesodermal differentiation. On day 2, cells were placed in RPMI+B27 without insulin and without CHIR99021. On days 3-4, cells were treated with 5 μM IWR-1 (Sigma) to inhibit Wnt pathway signaling and induce cardiogenesis. On days 5-6, cells were removed from IWR-1 treatment and placed in RPMI+B27 without insulin. From day 7 onwards, cells were placed in RPMI+B27 with insulin until beating was observed. At this point, cells were glucose-starved for 3 days with RPMI (no glucose)+B27 with insulin to purify the hiPSC-CMs, as CMs can selectively metabolize fatty acids as an alternate source of cellular energy (Tohyama et al., 2013). Following purification, cells were cultured in RPMI 1640+B27 with insulin. When replating hiPSC-CMs for downstream use, cells were dissociated with 0.25% trypsin-EDTA (Life Technologies) into a single-cell suspension and seeded on Matrigel-coated "BioCell" 6-well plates customized for microgravity cell culture (BioServe Space Technologies).

Microgravity Cell Culture. hiPSC-CMs within the BioCells were cultured in a high-nutrient variant of cardiomyocyte maintenance media (RPMI 1640 with L-GlutaMAX + B27 with insulin + 15 mM Hepes + 5% PenStrep). Sterile syringes containing 10 mL of high nutrient culture media were attached to sterile ports on each well of the BioCell and pumped up and down 15 times to mix the fresh media with the spent media, producing an approximate 80% media change. Media changes for ground controls were completed in the same manner, with timing replicated exactly on a six-hour delay from the ISS.

Ca^{2+} Imaging. Three days after splash-down of flight samples from the ISS, hiPSC-CMs were treated with 5 μM Fluo-4 AM and 0.02% Pluronic F-127 (Molecular Probes) in Tyrode's solution for 15 minutes at 37°C. Cells were washed with Tyrode's solution afterward. Ca^{2+} imaging to examine calcium flux during hiPSC-CM contractility was conducted using a Zeiss LSM 510Meta confocal microscope (ZEISS) (20× Plan Apochromat NA 0.8). Spontaneous Ca^{2+} transients were obtained at 37°C using a single-cell line scanning mode (512 pixels*1920 lines). Ca^{2+} images were analyzed with a custom-made MATLAB algorithm.

Immunofluorescence and Microscopy. Immunostaining was performed according to previous protocols (Sharma et al., 2014). Briefly, membranes were cut out of the BioCell plates and placed in standard 6-well culture plates (Corning). Cells were fixed using 4% paraformaldehyde and treated with 0.1% TX-100 in PBS to permeabilize cell membranes. Primary antibodies for cardiac troponin T (Abcam AB45932) and cardiac alpha-actinin (Sigma A7811) were diluted 1:200 in 2% goat serum in PBS and incubated on the cells overnight. Secondary antibodies conjugated with fluorophores (Invitrogen A11029, A11037) were diluted 1:500 in 2% goat serum in PBS and incubated on the cells for 2 hours. Cell nuclei were stained using NucBlue™ Fixed Cell ReadyProbes™ Reagent (Invitrogen R37606) diluted in PBS for 20 minutes. Membranes were fixed to a coverslip using ProLong™ Gold Anti-Fade Reagent (Invitrogen P36931). Imaging was performed using a LSM710 confocal microscope (ZEISS) through the Stanford Neuroscience Microscopy Service facility.

Live Imaging and Contractility Assessment. Cells were imaged 9 and 16 days into space flight using a Nikon Eclipse TS100 microscope (ISS) and Leica DM IL LED microscope (ground). One plate from each group (flight vs ground) was used for imaging. Plates were removed from the incubator, imaged, and returned to the incubator on the same schedule, with the groundside control plate on a six-hour delay. Fifteen second videos were divided into regions of interest (ROI) containing one or more CM patches, with ROI size consistent within each video. ROIs were chosen to maximize covered beating cell area and minimize coverage of non-beating areas. ROI videos were converted to image sequences with a frame rate of 15 frames per second. Image sequences were analyzed using a MATLAB program described previously (Huebsch et al., 2016). Each contraction velocity trace was manually matched to the respective video and ROI to ensure the traces matched cardiomyocyte contraction.

RNA-sequencing Gene Expression Analysis. RNALater (Thermo Fisher) was used to preserve flight samples designated for downstream RNA-sequencing analysis. Samples preserved in RNALater were stored at 4°C until return to our laboratory, when RNA was isolated from preserved wells in the BioCells using RNeasy kit (Qiagen) following the manufacturer's protocol. DNase treatment was performed using RNase-free DNase kit (Qiagen). All RNA samples had RNA integrity number ≥ 8.9 and concentration ≥ 48 ng/µL (Agilent 2100 Bioanalyzer). Library prep and sequencing were performed by BGI with 30-40 million paired-end 100bp reads per sample on the Illumina HiSeq platform. The raw reads were aligned by HISAT2 (https://ccb.jhu.edu/software/hisat2/index.shtml)(Kim et al., 2015) to human genome (hg38). The aligned reads were quantitated by FeatureCounts (http://bioinf.wehi.edu.au/featureCounts/) with the annotation of ENSEMBL 85. The normalization and differentially expressed genes test were implemented by DESeq2 (https://bioconductor.org/packages/release/bioc/html/DESeq2.html) (Liao et al., 2014; Love et al., 2014). DESeq2 data were analyzed using Qlucore Omics Explorer Software. For the motif enrichment analysis, the promoter sequences of differentially expressed genes (upstream 400bp, downstream 100bp) were extracted from the human genome and fed to Hypergeometric Optimization of Motif EnRichment (HOMER) software (Heinz et al., 2010). The enriched motifs were then compared with the curated HOMER motif database. Database for Annotation, Visualization, and Integrated Discovery (DAVID) Bioinformatics Resources Functional Annotation Tool (version 6.8 - https://david.ncifcrf.gov/summary.jsp) was used to determine the functional annotation clusters of differentially expressed genes between each group, with differential gene lists based on a two-tailed Student's t-test with $p \leq 0.05$ (Huang et al., 2009a, 2009b). The Venn diagram of differentially expressed genes for each comparison was created using a tool through VIB/UGent Bioinformatics & Evolutionary Genomics (http://bioinformatics.psb.ugent.be/webtools/Venn/).

Statistical Methods. Data presented as mean ± SEM. Comparisons were conducted via Student's t-test with significant differences (*) defined by $p < 0.05$.

Supplemental References

Churko, J.M., Burridge, P.W., and Wu, J.C. (2013). Generation of human iPSCs from human peripheral blood mononuclear cells using non-integrative Sendai virus in chemically defined conditions. In Cellular Cardiomyoplasty: Methods in Molecular Biology (Methods and Protocols), pp. 81–88.

Heinz, S., Benner, C., Spann, N., Bertolino, E., Lin, Y.C., Laslo, P., Cheng, J.X., Murre, C., Singh, H., and Glass, C.K. (2010). Simple combinations of lineage-determining transcription factors prime cis-regulatory elements required for macrophage and B cell identities. Mol. Cell *38*, 576–589.

Huang, D.W., Sherman, B.T., and Lempicki, R.A. (2009a). Bioinformatics enrichment tools: paths toward the comprehensive functional analysis of large gene lists. Nucleic Acids Res. *37*, 1–13.

Huang, D.W., Sherman, B.T., and Lempicki, R.A. (2009b). Systematic and integrative analysis of large gene lists using DAVID bioinformatics resources. Nat. Protoc. *4*, 44–57.

Huebsch, N., Loskill, P., Deveshwar, N., Spencer, C.I., Judge, L.M., Mandegar, M.A., B. Fox, C., Mohamed, T.M.A., Ma, Z., Mathur, A., et al. (2016). Miniaturized iPS-cell-derived cardiac muscles for physiologically relevant drug response analyses. Sci. Rep. *6*, 24726.

Kim, D., Langmead, B., and Salzberg, S.L. (2015). HISAT: a fast spliced aligner with low memory requirements. Nat. Methods *12*, 357–360.

Lian, X., Hsiao, C., Wilson, G., Zhu, K., Hazeltine, L.B., Azarin, S.M., Raval, K.K., Zhang, J., Kamp, T.J., and Palecek, S.P. (2012). Robust cardiomyocyte differentiation from human pluripotent stem cells via temporal modulation of canonical Wnt signaling. Proc. Natl. Acad. Sci. *109*, E1848–E1857.

Liao, Y., Smyth, G.K., and Shi, W. (2014). featureCounts: an efficient general purpose program for assigning sequence reads to genomic features. Bioinformatics *30*, 923–930.

Love, M.I., Huber, W., and Anders, S. (2014). Moderated estimation of fold change and dispersion for RNA-seq data with DESeq2. Genome Biol. *15*, 550.

Sharma, A., Marceau, C., Hamaguchi, R., Burridge, P.W., Rajarajan, K., Churko, J.M., Wu, H., Sallam, K.I., Matsa, E., Sturzu, A.C., et al. (2014). Human induced pluripotent stem cell-derived cardiomyocytes as an in vitro model for coxsackievirus B3-induced myocarditis and antiviral drug screening platform. Circ. Res. *115*, 556–566.

Tohyama, S., Hattori, F., Sano, M., Hishiki, T., Nagahata, Y., Matsuura, T., Hashimoto, H., Suzuki, T., Yamashita, H., Satoh, Y., et al. (2013). Distinct metabolic flow enables large-scale purification of mouse and human pluripotent stem cell-derived cardiomyocytes. Cell Stem Cell *12*, 127–137.